TOPOLOGY OPTIMIZATION OF HAND BRAKE LEVER USING NUMERICAL AND EXPERIMENTAL APPROACH

Avilasha B. G.[1] and Dr. Ramakrishna D.S.[2]
[1]Assistant Professor, Mechanical Engineering Department, Dayanandasagar College of Engineering Visvesvaraya Technological University, Belagavi -590018, Karnataka, India
[2]HOD and Professor (Retired), Mechanical Engineering Department, Jawaharlal Nehru College of Engineering Visvesvaraya Technological University, Belagavi -590018, Karnataka, India
[1]avilashabgr9@gmail.com and [2]ramak_ds@yahoo.com

ABSTRACT
This research is dedicated to the application of experimental topology optimization to improve the design of the hand brake lever, a mechanically intricate component. The primary objective is to minimize the mass of the hand brake lever while ensuring it maintains structural integrity and performance. Photoelasticity experiments are utilized to visualize and analyze stress patterns in birefringent materials, providing experimental confirmation of the stress distribution in the optimized design. The study begins by formulating the topology optimization problem, defining the design space, objective function, and constraints. Altair Optistruct topology optimization tool is employed for computational analysis, and Finite Element Analysis is conducted to simulate the structural response of both the initial and iteratively optimized models. The latter is validated through the photoelasticity method.

The optimization process involves using the density method, iteratively updating material distribution to enhance the objective function while adhering to specified constraints. The results demonstrate the effectiveness of topology optimization, achieving a significant 24.88% reduction in weight while preserving the structural integrity of the hand brake lever. Photoelasticity emerges as a crucial method for experimentally verifying stress distribution. The combination of computational simulations and experimental validation through photoelasticity presents a comprehensive approach to optimizing and validating mechanical components. This approach showcases the potential for efficient design improvements in real-world applications.

Index Terms – Hand brake lever, optimization, Photoelasticity, Stress distribution. Structural integrity, Topology Weight reduction,

INTRODUCTION
Topology optimization has gained significant attention in engineering and design fields for creating lightweight and efficient structures. If the design is susceptible to rework, leading to unexpected increase in costs. In the realm of topology optimization, addressing the interplay between density and stress poses a considerable challenge, a task that has been a source of difficulty in our research domain since the seminal work of Bendsoe M, Diaz A, Kikuchi N [1]

Notably, [2] [3] presented a shape and topology optimization using homogenization method which distributes the density as zero and one for plane structures using algorithms. The density approach of topology optimization has implemented to study the viscothermal acoustic and boundary loading problems which boundary density eliminator by PDE.[4], [5]

[6] the elastic stress tensor was assumed to depend linearly on density, the values are controlled by explicit constrained, the convergence of the structure achieved by finite element (FE) discretization optimization method solved by sequential approximations. [7]–[9]evident that the computational method of topology optimization using density approach, the finite element method with mesh refinement to achieve the topologies of different structures among different methods [2] The finite element methods and algorithms are widely used for the topology optimization of different applications, the fine grained matrix free conjugate gradient solver for finite

element analysis(FEA) using graphic processing unit (GPU) which leads to massive parallel processing of the degree of freedom for the analysis [10].

The isotropic material distribution is the key factor for achieving light wight topologies of the structures and components. The design and structural optimization stand out for the additive manufacturing of the components. The review on this explains the [11] generative designs for the optimal topologies and the commercial software's are introduced to enhance the quality of the work.

The literature also evident for the non-linear analysis of the components [12] the volume preserving density filter method is discussed in the paper, the topology optimization using the continuous density field and adaptive mesh refinement and boundaries with checkboard concept of density values.[8] All evident to minimize the compliance of the components. The finite element analysis opted for the non-conforming mesh refinement for the higher order finite elements which follows the density method of algorithms for the analysis.[13].

Notably with [14] commercial software tools like Genesis, MSC Nastran and Altair Optistruct optimization tools are investigated by considering the different problem statement, the results shows that the Genesis gives the best in computational time while Optistruct gives the excellent optimal solution in shape and topology optimization. the Nastran gives the good solution in topography and shape. [15] This study proposes a more computationally efficient approach to structural optimization by utilizing a Krylov subspace iterative solver to approximate the solution of analysis equations. The key is to tailor convergence criteria to the optimization objective and design sensitivities. [16] The study proposes efficient topology optimization schemes using the multiscale finite element method (MsFEM), integrating SIMP and level-set techniques. The approach is validated through 2D and 3D examples, demonstrating effectiveness and efficiency in addressing complex topology optimization problems.

COMPUTATIONAL TOPOLOGY OPTIMIZATION

Topology optimization relies on mathematical optimization and structural mechanics to iteratively adjust material distribution, aiming to improve an objective function. Illustrated with a flowchart, Figure 1 the process involves defining a design problem, setting constraints, and optimizing parameters. Using a lever example, considerations include design and non-design areas, geometric and material constraints, and an objective of minimizing weight. The overall goal is to achieve more efficient and lightweight structural designs through this optimization process.

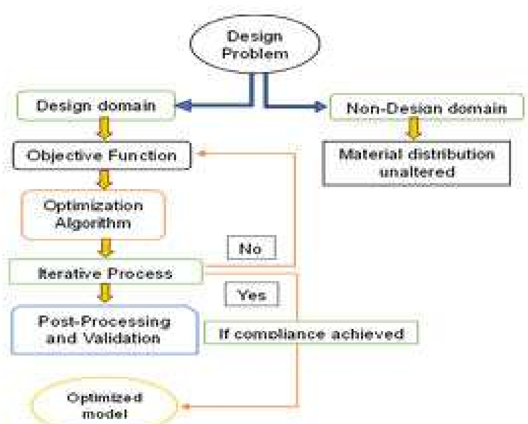

Figure 1: Process Flow chart of Topology Optimization.

The paper focuses on topology optimization using the density method of topology optimization, Altair Hyperwork's Optistruct software is employed, utilizing the density method for analysis. The study aims to explore optimal material distribution within a design space and non-design to achieve improved structural performance. The paper discusses the general formulation for optimal structural design in a linear elastic body, with the objective of minimizing compliance through iterative updates of material distribution. The general formulation for optimal structural design in a linear elastic body is examined in the paper. It considers a mechanical element occupying a domain Ω, which is subjected to both body forces (f) and tractions (t). The objective is to find the optimal design for minimum compliance, denoted as L(v), where v represents the material distribution.

$a_E(u, v) = \int_{\Omega}^{0} E, \in (u)dx$ (1)

$L(v) = \iint_{\Omega}^{0} f, v, dx + \int_{t}^{0} f.v.ds$ (2)

the indicator function for the part Ω_m of Ω that is occupied by the material. The function of the spatial variable x∈Ω, the material distribution occupied by the element.[12].

$X(x) = \int_{0}^{1} if\ x \in \Omega m$ (3)

The optimization process continues iteratively until convergence is achieved, indicating that further iterations do not significantly enhance the design. The finalized optimized design reflects an efficient material layout that satisfies the predefined objectives and constraints, resulting in a mechanically optimized structure.

The paper focuses on topology optimization applied to the hand brake lever of the racing cars, considering loading conditions. The lever is meshed with 3D tetrahedron elements, and material assignment is determined by stress levels. Figures 2 illustrate specified boundary conditions, providing a clear overview of loading and constraints in the study.

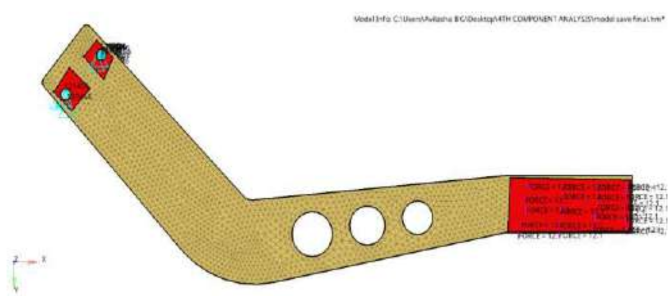

Figure 2: Boundary conditions.

The Optistruct analysis, utilizing a density approach, iteratively identifies lower stress regions in the hand brake lever structure, achieving an optimal solution in 17 iterations. This results in a 24.88% reduction in mass, demonstrating the effectiveness of the optimization process in improving structural performance while significantly decreasing mass.

EXPERIMENTAL TOPOLOGY OPTIMIZATION

Photoelasticity is an experimental technique utilized in engineering and material science for stress analysis. This method involves examining the optical properties of materials under mechanical loading to visualize and analyze stress distribution. In the context of this study, the photoelasticity method is employed as a topology optimization technique to achieve the optimal solution for the lever.

The principle of photoelasticity is based on the observation that certain materials exhibit birefringence when subjected to mechanical stress. Birefringence refers to a material's property to split incident light into two orthogonal polarization components, leading to the formation of fringe patterns. Commonly used materials for photoelastic experiments include epoxy, shaped into the desired specimen geometry.

The photoelastic experiment setup comprises a light source (S), polarizers (P), first quarter wave plate (Q1), model placement (M), second quarter wave plate (Q2), and an analyzer (A) as depicted in Figure 4. A circular polariscope employs a white light source, while a sodium vapor light source is used in stress analysis to achieve a specific light field arrangement, causing fringes to appear darker. A linear polarizer is utilized to polarize the light toward the first quarter wave plate. The first and second quarter wave plates convert the light into fast and slow axes, oriented at 45 degrees to each other. The fast and slow components pass through the model and second quarter wave plate, and fringes are observed from the analyzer.

When mechanical stress is applied to photoelastic material, it undergoes stress-induced birefringence, leading to a phase difference and the formation of fringe patterns. The zero-order fringe, appearing at the centre under uniform or absent stress, is crucial for determining the unwrapped fringe order. This understanding provides valuable insights into the stress state, contributing to informed decisions about the design and performance of structures in the study.

In the experimentation phase, a prototype of the lever is constructed using epoxy resin, a material known for exhibiting birefringence properties. The model is then subjected to loading conditions defined the boundary conditions. To facilitate experimentation, the lever is scaled down to a 1:2 ratio. It's worth noting that the stress distribution remains unaffected by this scaling.

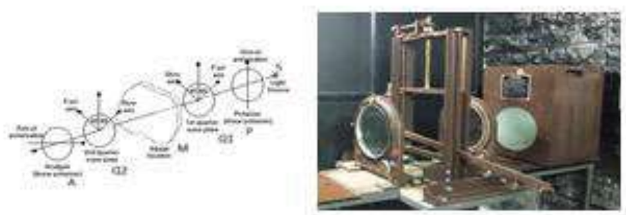

Figure 3: A) Polariscope arrangement (b) Experiment set up

By leveraging the birefringence property of the epoxy resin, the photoelasticity method allows for a visual and analytical assessment of stress distribution. This information is crucial for guiding the iterative topology optimization process, ultimately leading to a design that meets the defined objectives while satisfying constraints related to stress, structural integrity, and performance. The both loading conditions are considered for initial iteration of lever, the fringe patterns are recorded and captured for the analysing the fringe orders. This study focuses on the zero order fringes and lower order fringes which exhibits lower principal stress difference ($\sigma1$-$\sigma2$).

The magnitude of principal stress difference (σ_1-σ_2) at any point can be determined from the formula (4).

$$\sigma1-\sigma2 = \frac{N\, f\sigma}{h} \qquad (4)$$

N- isochromatic fringe order at point under consideration, fσ material fringe value of model material, h- thickness of the model. The isochromatic fringe order 'N' is determined by observing the fringe pattern in the polariscope. The experimental study shows that, the principal stress difference at a point $\sigma1$-$\sigma2$=0 when isochromatic fringes and 'N' is '0' at point. This can happen under two conditions: 1) when both principal stresses are zero, and 2) when both the principal stresses are of the same magnitude and sign. Whether the point under consideration has '0' stress, a material can be removed using result from finite element analysis.

In the presence of a polariscope (Fig 4(b)), a combination of polarizers and analysers, viewing the loaded specimen reveals fringe patterns formed due to stress-induced birefringence. Concurrently, Finite Element Method (FEM) analysis is conducted to identify lower stress regions, providing validation for the experimental results. Lower order fringes are identified, leading to the removal of material in the initial iterations for both loadings. This process is iteratively repeated until the optimized solution is achieved.

The optimization of the lever involves two iterations to achieve the optimal shape, with increased fringes observed after the second iteration. Feasible results are discussed, and a comprehensive validation is conducted through comparisons with Optistruct, experimental data, and FEM analysis. This multifaceted approach, combining experimental observations, simulations, and FEM analysis, ensures a thorough understanding of the lever's behaviour under different loading conditions. The iterative process allows for adjustments to material distribution, leading to a final optimized design. Photoelasticity proves valuable for analysing stress distribution in complex structures, offering visual insights into material behaviour.

RESULTS AND DISCUSSIONS

The use of photoelasticity in topology optimization provides valuable insights into stress distribution and design behaviours. Typically, discussions involve comparing experimentally observed stress patterns with the predicted stress distribution from the optimized design. This comparison enhances the understanding and validation of the topology optimization process.

In this study, Altair's Optistruct software is employed to compare the optimal solution of the lever, considering boundary conditions (Fig 1). The software utilizes the density method of topology optimization, and the results are plotted over 17 iterations. Convergence is achieved at the 15th and 17th iterations for load. The optimal solutions and density distribution of the optimized model from Optistruct are illustrated in Figure 4. Comparing predicted stress distribution with experimentally observed patterns through photoelasticity and Optistruct enables a thorough examination. Correlating these findings boosts researchers' confidence in the accuracy of the topology optimization process. This integrated approach, combining experimental data and computational simulations, enhances understanding of the optimized lever's structural behaviours under various loading conditions.

Fig 4 shows density distribution plots are presented for each element in the optimized lever. The assignment of density values follows a specific criterion: density 1 is assigned to elements experiencing higher stress levels, while zero and lower density values are assigned to elements experiencing lower stress levels. This density distribution illustrates the optimized solution achieved through the topology optimization process.

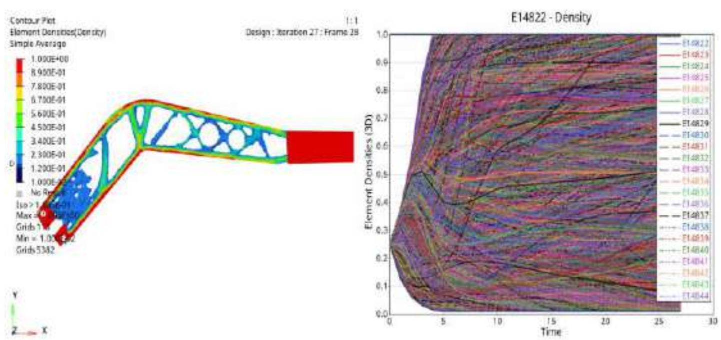

Figure 4: density plot

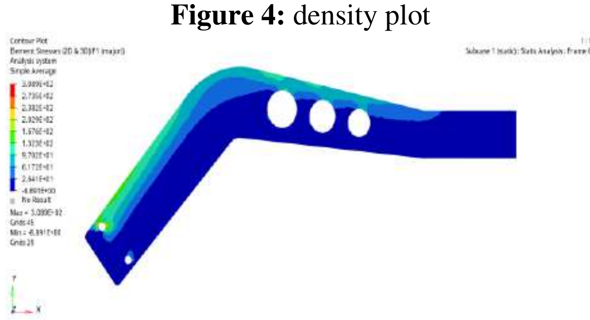

Figure 5: Principal stress before optimization

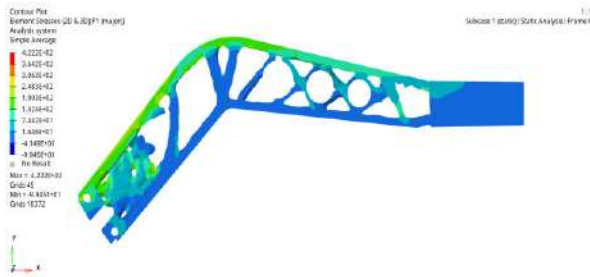

Figure 6: Principal Stress After Optimization

The study of principal stresses is a critical aspect of achieving the optimal solution for the lever. considered to investigate the optimal solutions. The principal stress values of before and after optimization are depicted in Fig 5 and 6, showing values 308.2 MPa, and 422.2Mpa respectively.

The stress plots depict the stress distribution in each element, highlighting lower stress regions. For a more detailed presentation of the results, stresses and displacements are tabulated. Table-1 provides a summary of the results obtained from Optistruct, offering a comprehensive overview of the structural performance of the optimized lever under boundary conditions. The tabulated results serve as a quantitative reference for the achieved improvements in stress distribution and displacement after the optimization process.

Table 1: Optistruct Results

Sl No	Load N	Principal Stress before TO Mpa	Principal Stress after TO Mpa	Weight reduction%
1	490	308.2	422.2	24.88

The paper advocates the application of an experimental approach to topology optimization of levers. The experimentation involves an initial iteration where conditions are applied to the prototype. This suggests that different loading scenarios are being considered to understand their impact on the lever's behaviours. The study focuses on zero-order and lower-order fringes during the analysis. Fringes in photoelasticity represent regions of different stress levels. Figures 7 (a) show the identified zero and lower-order fringes of initial iteration. Initial iteration stress is 30.28Mpa.

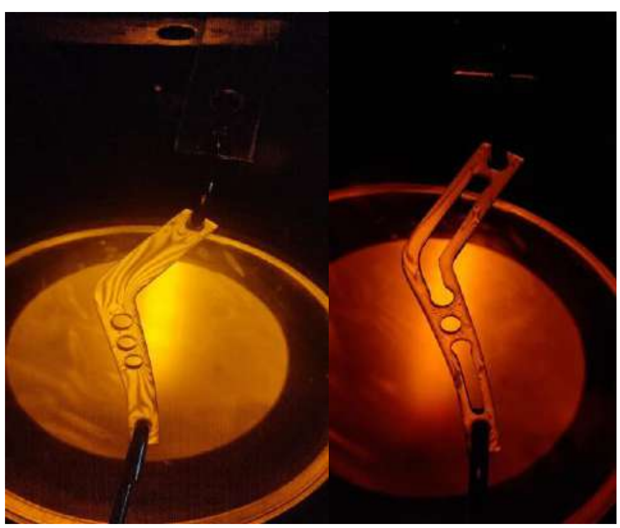

FIGURE 7: (a) initial iteration (b) First iteration.

The first iteration is carried out under two different loads, referred to as load-1 and load-2. This implies that you are applying external forces to the model to induce stress. first iteration of photoelasticity, specifically focusing on the zero-order and lower-order fringes. Isochromatic fringes are observed, which indicate areas of equal stress. Lower-order fringes typically correspond to lower stress levels. Figures 7(b) display the experimental results. Isochromatic fringes are visible, and lower-order fringes are observed at centre of the lever. The stress at first iteration is 65.82Mpa.

The Finite Element Method (FEM) analysis is conducted in the initial iteration to validate the principal stress at a specified point, as depicted in Figures 8 and 9. This analytical approach provides stress values at each element, offering support and corroboration for the experimental findings. These plots serve as visual representations of the distribution of displacement and principal stress throughout the analysed structure. The analysis results are tabulated in Table-1.

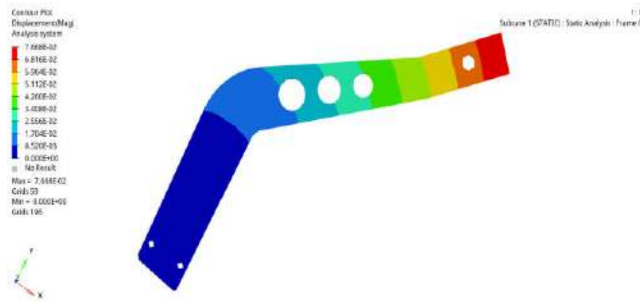

Figure 8: Displacement initial iteration.

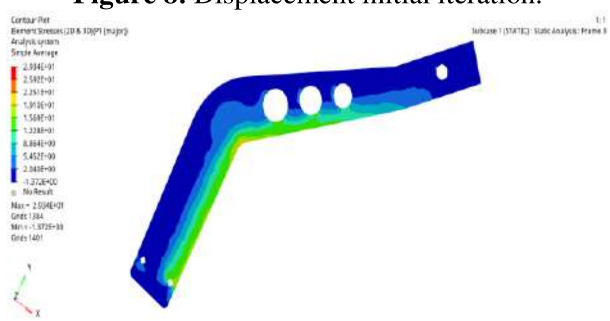

Figure 9: P1 at initial iteration.

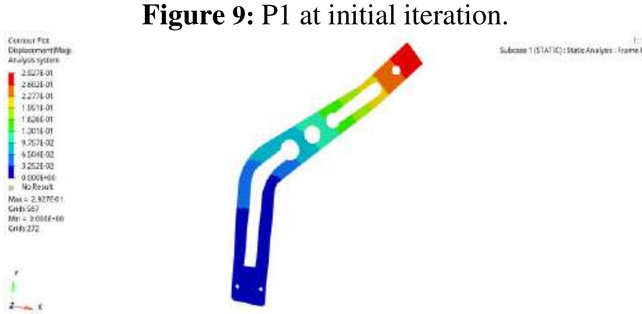

Figure 10: Displacement at first iteration.

Figure 11: P1 at first iteration.

Table 2: FEM analysis

Sl No	Displacement mm	Principal Stress Difference Mpa
Initial iteration	0.071	30.25
First iteration	0.29	62.32

The comparison of the initial, first iterations of Finite Element Method (FEM) analysis is conducted. The graph illustrates that the principal stress is lower at distinct nodal values. The discernible drop in the graph signifies regions of lower stress, indicating areas where material removal could be considered for optimization purposes

Table 3: Comparison

Iteration	FEM		Photoelasticity	
	Displacement mm	Stress Mpa	Displacement mm	Stress Mpa
Initial iteration	0.071	30.25	0.002	32.2
1^{st} iteration	0.29	62.32	0.002	70.233
Mass Reduction	24.88%			

For further clarity, the comparison of principal stress values is systematically presented in Table 8. This tabulated data provides a comprehensive overview of how the principal stress values align between the experimental observations, computational optimization method, and FEM analysis. The consistent adherence to allowable stress limits, coupled with substantial mass reduction, underscores the success of the optimization efforts in enhancing the lever's performance while maintaining its structural integrity.

CONCLUSION

The integration of topology optimization with photoelasticity offers a comprehensive approach to designing and analyzing optimized structures. By combining computational techniques like Optistruct with experimental stress analysis, a thorough understanding of the performance and behaviors of optimized designs is achieved. The use of photoelasticity in topology optimization allows for informed decisions about the entire component's density distribution.

- Experimental photoelastic analysis provides insights into induced stress, with maximum stress reaching 70.60 MPa in initial, first, revealing principal stress distribution through lower and higher order fringes.

- Computational analysis focuses on the design space, lacking consideration for material removal in the non-design space. The experimental method overcomes this limitation, offering complete accessibility for material optimization.
- The study emphasizes that the use of photoelasticity as a topology optimization technique yields superior results. By comparing results, a feasible solution with a substantial 24.88% mass reduction is achieved. This compelling outcome highlights the efficacy of the photoelasticity method as a valuable tool for achieving topology optimization in various applications.

ACKNOWLEDGMENTS

I acknowledge everyone who directly and indirectly involved in this research work.

REFERENCES

[1] M. P. Bendsøe, A. Díaz, and N. Kikuchi, "Topology and Generalized Layout Optimization of Elastic Structures," Topology Design of Structures, pp. 159–205, 1993, doi: 10.1007/978-94-011-1804-0_13.

[2] K. Suzuki and N. Kikuchi, "A homogenization method for shape and topology optimization," Comput Methods Appl Mech Eng, vol. 93, no. 3, pp. 291–318, 1991, doi: 10.1016/0045-7825(91)90245-2.

[3] M. P. Bendsøe and N. Kikuchi, "Generating optimal topologies in structural design using a homogenization method," Comput Methods Appl Mech Eng, vol. 71, no. 2, pp. 197–224, 1988, doi: 10.1016/0045-7825(88)90086-2.

[4] C. Wang and X. Qian, "A density gradient approach to topology optimization under design-dependent boundary loading," J Comput Phys, vol. 411, Jun. 2020, doi: 10.1016/j.jcp.2020.109398.

[5] A. Mousavi, M. Berggren, and E. Wadbro, "Extending material distribution topology optimization to boundary-effect-dominated problems with applications in viscothermal acoustics," Mater Des, vol. 234, Oct. 2023, doi: 10.1016/j.matdes.2023.112302.

[6] T. Borrvall and J. Petersson, "Topology optimization using regularized intermediate density control," Comput Methods Appl Mech Eng, vol. 190, no. 37–38, pp. 4911–4928, Jun. 2001, doi: 10.1016/S0045-7825(00)00356-X.

[7] E. Aranda, J. C. Bellido, and A. Donoso, "Toptimiz3D: A topology optimization software using unstructured meshes," Advances in Engineering Software, vol. 148, Oct. 2020, doi: 10.1016/j.advengsoft.2020.102875.

[8] A. B. Lambe and A. Czekanski, "Topology optimization using a continuous density field and adaptive mesh refinement," Int J Numer Methods Eng, vol. 113, no. 3, pp. 357–373, Jan. 2018, doi: 10.1002/NME.5617.

[9] K. Svanberg, "The method of moving asymptotes—a new method for structural optimization," Int J Numer Methods Eng, vol. 24, no. 2, pp. 359–373, 1987, doi: 10.1002/NME.1620240207.

[10] J. Martínez-Frutos, P. J. Martínez-Castejón, and D. Herrero-Pérez, "Fine-grained GPU implementation of assembly-free iterative solver for finite element problems," Comput Struct, vol. 157, pp. 9–18, Jun. 2015, doi: 10.1016/j.compstruc.2015.05.010.

[11] J. Plocher and A. Panesar, "Review on design and structural optimisation in additive manufacturing: Towards next-generation lightweight structures," Mater Des, vol. 183, Dec. 2019, doi: 10.1016/j.matdes.2019.108164.

[12] S. Xu, Y. Cai, and G. Cheng, "Volume preserving nonlinear density filter based on heaviside functions," Structural and Multidisciplinary Optimization, vol. 41, no. 4, pp. 495–505, Apr. 2010, doi: 10.1007/S00158-009-0452-7.

[13] J. Červený, V. Dobrev, and T. Kolev, "Nonconforming mesh refinement for high-order finite elements," SIAM Journal on Scientific Computing, vol. 41, no. 4, pp. C367–C392, 2019, doi: 10.1137/18M1193992.

[14] W. han Choi, J. moon Kim, and G. J. Park, "Comparison study of some commercial structural optimization software systems," Structural and Multidisciplinary Optimization, vol. 54, no. 3, pp. 685–699, Sep. 2016, doi: 10.1007/S00158-016-1429-Y.

[15] O. Amir, M. Stolpe, and O. Sigmund, "Efficient use of iterative solvers in nested topology optimization," Structural and Multidisciplinary Optimization, vol. 42, no. 1, pp. 55–72, Jul. 2010, doi: 10.1007/S00158-009-0463-4.

[16] H. Liu, Y. Wang, H. Zong, and M. Y. Wang, "Efficient structure topology optimization by using the multiscale finite element method," Structural and Multidisciplinary Optimization, vol. 58, no. 4, pp. 1411–1430, Oct. 2018, doi: 10.1007/S00158-018-1972-9.

[17] T. P. Ribeiro, L. F. A. Bernardo, and J. M. A. Andrade, "Topology optimisation in structural steel design for additive manufacturing," Applied Sciences (Switzerland), vol. 11, no. 5, pp. 1–66, Mar. 2021, doi: 10.3390/APP11052112.

[18] O. Amir, M. P. Bendsøe, and O. Sigmund, "Approximate reanalysis in topology optimization," Int J Numer Methods Eng, vol. 78, no. 12, pp. 1474–1491, Jun. 2009, doi: 10.1002/NME.2536.

[19] S. Zhang, A. L. Gain, and J. A. Norato, "Stress-based topology optimization with discrete geometric components," Comput Methods Appl Mech Eng, vol. 325, pp. 1–21, Oct. 2017, doi: 10.1016/j.cma.2017.06.025.

[20] H. Emmendoerfer, K. Maute, E. A. Fancello, and E. C. N. Silva, "A level set-based optimized design of multi-material compliant mechanisms considering stress constraints," Comput Methods Appl Mech Eng, vol. 391, Mar. 2022, doi: 10.1016/j.cma.2021.114556.

[21] M. P. Bendsøe, A. R. Díaz, R. Lipton, and J. E. Taylor, "Optimal design of material properties and material distribution for multiple loading conditions," Int J Numer Methods Eng, vol. 38, no. 7, pp. 1149–1170, 1995, doi: 10.1002/NME.1620380705.